Extended Abstracts of the 18th (1986 International) Conference on Solid State Devices and Materials, Tokyo, 1986, pp. 45-48

A-3-3

Si/SrO/Si Heteroepitaxial Structure Formation by Molecular Beam Epitaxy

Yuichi Kado and Yoshinobu Arita

NTT Electrical Communications Laboratories

3-1 Morinosato Wakamiya, Atsugi-shi, kanagawa 243-01, Japan

SrO has been proposed for use as an insulating film with low dielectric constant (3.0) for a Si/insulator/Si heteroepitaxial structure. Epitaxial growth of SrO films onto Si substrates and the growth of Si films onto SrO/Si(111) structure have been achieved by molecular beam epitaxy(MBE). These SrO films possess a high breakdown field ($5X10^6$V/cm). It has been found from Rutherford backscattering/channeling (RBS/C) spectroscopy that the channeling minimum yield of the top Si layer behind the surface peak is 2.7%, which is comparable to that of bulk Si.

1. Introduction

Heteroepitaxial growth of single crystal films on Si substrates is of great interest in adding new functions to conventional Si-LSIs. In particular, Si/insulator heteroepitaxial structures stacked onto Si substrates are promising for use in the fabrication of silicon-on-insulator devices and three-dimensional integrated circuits. Previous studies using Spinel [1], BP [2], and CaF_2 [3] as single crystalline insulating films have been reported.

We searched systematically for new cubic insulating materials having lattice constants which yield less than about 5 % mismatch with those of Si and which easily form stoichiometric films. From the standpoint of device applications, SrO was selected for its several desired physical properties .

Bulk SrO has a lower dielectric constant (3.2) than conventional epitaxial insulating crystals, and a high melting point (2460 ℃). [4] In addition, it has a simple cubic, NaCl structure with a=5.140 Å[5] which is well suited for matching with crystalline Si. In this paper, properties of epitaxial SrO films grown on Si substrates and the formation of Si/SrO/Si(111) stacked structure by introduction of a Si-SPE layer are discussed. The crystalline quality of the top Si layers was investigated using a chemical etching method and Rutherford backscattering /channeling (RBS/C).

2. Experiments

The molecular beam epitaxy (MBE) apparatus in this experiment is equipped with ion pumping, turbo molecular pumping and in situ 10 KV reflection high energy electron diffraction (RHEED). The chamber base pressure is less than $5X10^{-10}$ Torr. The Si wafers were chemically cleaned and boiled in solutions of H_2SO_4:H_2O_2(4:1) to produce a thin surface oxide.[6] Prior to deposition, this oxide was removed in an ultra high vacuum chamber by heating the substrate.

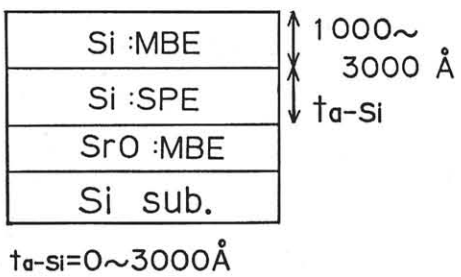

Fig.1 Cross-sectional view of a Si/SrO/Si structure.

In epitaxial growth of SrO films, SrO grains of 5N purity were evaporated as SrO molecules by an electron-gun (e-gun) onto Si substrates maintained at 650 ℃. The pressures maintained during evaporation were less than $5X10^{-7}$ Torr. The deposition rate of SrO films was approximately 1 Å /sec. In the deposition of Si overlayers, a Si source with 6N purity was evaporated in the same chamber by an e-gun onto the SrO/Si(111)

structure. The substrate temperatures during solid phase epitaxy (SPE) and top Si layer growth were 550 and 650 ℃, respectively. The pressures during Si evaporation were less than $7X10^{-9}$ Torr. The deposition rate of Si films was typically 0.3 Å/sec. A cross-sectional view of a Si/SrO/Si structure prepared in this experiment is shown in Fig.1.

The interdiffusion at the Si/SrO interfaces was analyzed by means of Auger electron spectroscopy (AES). The dielectric constant and the breakdown field of SrO films were evaluated from the C-V and I-V characteristics of an Al/SrO/Si(100) structure. The crystalline quality of the top Si layers on the SrO/Si(111) structure(Fig.1) was investigated using a Sirtl etching method. Furthermore, quantitative depth profiles of the crystalline perfection of the films were measured by RBS/C, using 2.0 MeV $^4He^+$ ions, with a variable scattering-angle detection system.

3. Results and Discussions

3.1 Growth of SrO films onto Si substrates and their electrical properties

RHEED patterns along the [1$\bar{1}$0] and [11$\bar{2}$] azimuths of SrO films grown on Si(111) at 650 ℃ are shown in Fig.2(a) and (b), respectively. The

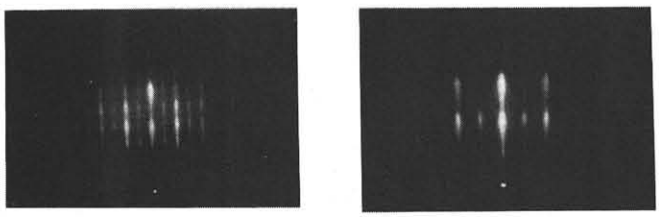

(a) (b)

Fig.2 RHEED patterns of 400 Å thick SrO films grown on Si(111) at 650 ℃. The incident electron beam was parallel to [1$\bar{1}$0] in (a), and [11$\bar{2}$] in (b) direction of the Si(111) substrates.

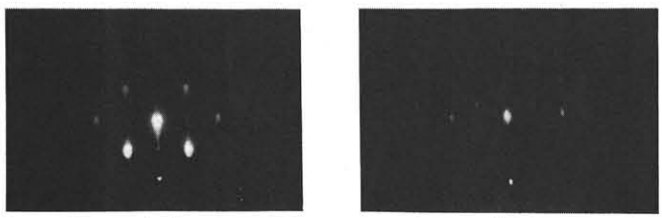

(a) (b)

Fig.3 RHEED patterns of 400 Å thick SrO films grown on Si(100) at 650 ℃. The incident electron beam was parallel to [011] in (a), and [013] in (b) direction of the Si(100) substrates.

epitaxial relationship derived from these patterns and RBS/C measurements is (111)SrO//(111)Si and [1$\bar{1}$0]SrO//[$\bar{1}$10]Si. These results indicate that SrO films on Si(111) have crystal orientations rotated 180° about the normal to the substrates (Type B).[7] Fig.3(a) and (b) show RHEED patterns along the [011] and [013] azimuths of SrO films grown on Si(100) at 650 ℃. The relationships (100)SrO//(100)Si and [011]SrO//[001]Si appear to exist. However, many extra spots were observed for SrO films grown on Si(100) at initial growth stages.

These results suggest that the crystalline quality of SrO films grown on Si(100) is poorer than that of the films grown on Si(111). Therefore, it is expected that high quality Si layer grown on SrO/Si structure can be accomplished more easily on SrO/Si(111) structure than on SrO/Si(100) structure.

Typical C-V characteristics of an aluminum/400 Å thick SrO layer/Si(100) structure are shown Fig.4. The dielectric constant was about 3.0. The interface charge density without H_2 treatment was approximately $2X10^{11}$ cm^{-2}. Moreover, the breakdown field of this same structure evaluated from I-V characteristics was $5X10^6$ V/cm.

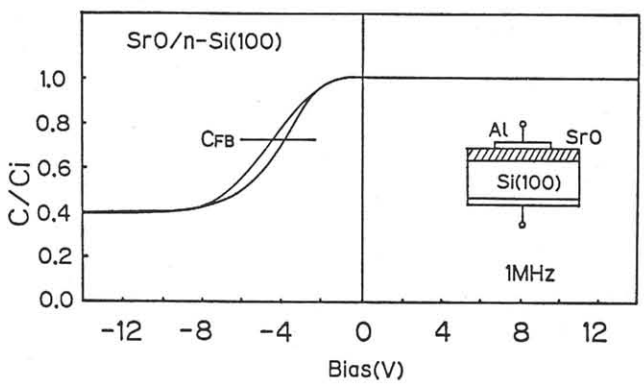

Fig.4 C-V characteristics of the MIS structure.

3.2 Growth of Si films onto the SrO/Si(111) structure

The sequence of RHEED patterns obtained during growth of top Si layers onto SrO/Si(111) structure is shown in Fig.5. Before Si deposition the patterns along the [110] azimuth of the SrO layer showed a clear streaked Pattern (a) indicating successful epitaxial growth. The halo-pattern after deposition of amorphous Si is shown

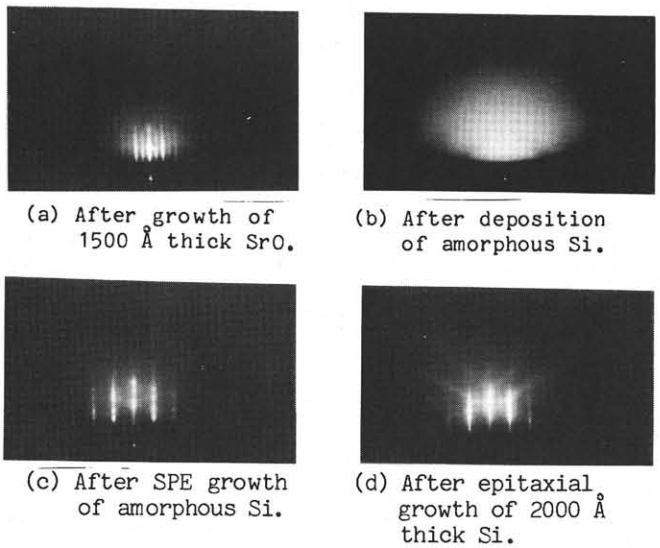

(a) After growth of 1500 Å thick SrO.

(b) After deposition of amorphous Si.

(c) After SPE growth of amorphous Si.

(d) After epitaxial growth of 2000 Å thick Si.

Fig.5 The sequence of 10KV-RHEED patterns along [1$\bar{1}$0]azimuth obtained during growth of top Si layers onto SrO/Si(111) structure.

in (b). After SPE growth of the amorphous Si layer Pattern (c) was obtained, which contained extra spots corresponding to the existence of {111} twins. These extra spots became weaker as the MBE-overgrown Si film thickness increased. After about 2000 Å thick Si layer growth on the SPE layer, these extra spots disappeared and a clear streaked 1X1 Pattern (d) appeared.

An Auger depth profile for the Si(1000 Å)/SrO(400 Å)/Si(111)structure [See Fig.1] without SPE layer and with SPE layer whose thickness is greater than 100 Å are shown in Fig.6(a) and (b), respectively. Samples without an SPE layer showed Sr and O-segregation on the top Si layers and interdiffusion at the top-Si/SrO interfaces [See Fig.6(a)]. On the other hand, Sr-segregation and noticeable interdiffusion at the interfaces were not observed for samples with SPE layer (b). This result indicates that interdiffusion at the top-Si/SrO interfaces could be suppressed by introducing an SPE layer.

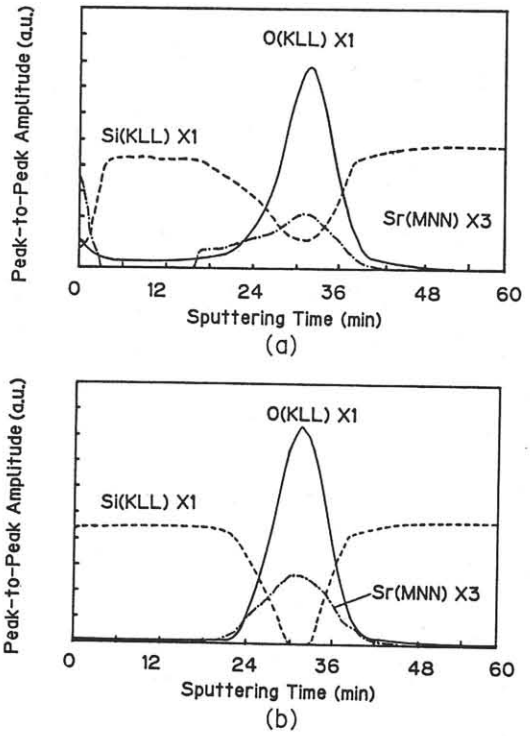

Fig.6 Auger depth profiles for the Si(1000 Å)/SrO(400 Å)/Si(111) structure without SPE layer (a) and with 100 Å thick SPE layer (b)

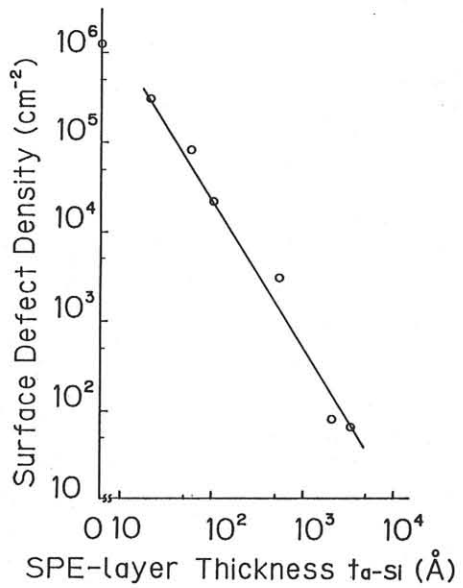

Fig.7 Relationship between the surface defect density and SPE-layer thickness (t_{a-Si})

3.3 Crystalline quality of the top Si layers

The crystalline quality of the top Si layer on the SrO/Si(111) structure(Fig.1) was investigated using a Sirtl etching method. The etching rate of the Sirtl etching solution was 250 Å/sec for bulk Si. Etching time was 4-10 sec for the samples. The defects revealed by etching were observed through an optical interference microscope. The defect density depended on the depth from the surface. Surface defects are defined as defects which exist at a depth less than 1000 Å from the surface and which appear by etching. The surface defect density is shown as a function of the SPE-layer thickness (t_{a-Si}) in Fig.7 . It is found from this figure that the surface defect density decreases as the SPE-layer thickness increases and that the formation of SPE-layer whose thickness is greater than 2000 Å

results in significant suppression of the defect density near the top-Si surface.

The surface defect observed from samples with 0-50 Å thick SPE layer is thought to be caused by Sr and O-segregation on top of the Si films. Because, for samples with 0-50 Å thick SPE layer, Sr and O-segregation on the surface was actually detected by AES analysis. The cause of surface defect for samples with SPE-layer whose thickness is greater than 100 Å is also thought to be Sr and O-diffusion into the top-Si layer, but these diffusions could not be detected by AES analysis.

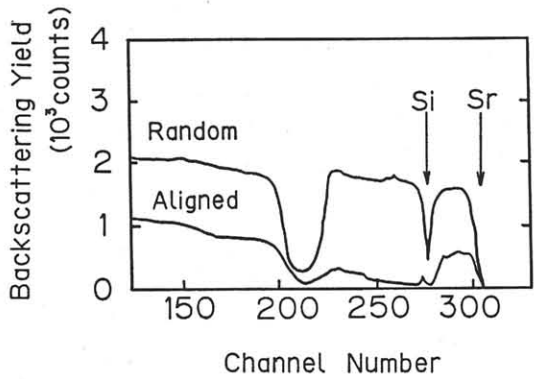

Fig.8 Random and aligned <111> backscattering spectra of Si(5000 Å)/SrO(1500 Å)/Si(111) structure (t_{a-Si}=2000 Å, See Fig.1). This spectrum was taken with 2 MeV $^4He^+$ ions.

The result of <111> channeling spectra of 2.0 MeV $^4He^+$ ions from a Si/SrO/Si(111) structure (t_{a-Si}=3000 Å) is illustrated in Fig.8. The channeling minimum yield χ_{min} in the top-Si film is about 0.04 near the surface and about 0.12 near the interface in large scattering-angle geometry (scattering-angle=170°). In addition, RBS/C analysis along the <111>,<110> and <114> axes was also made of this sample , which showed that the top-Si layer is again rotated 180° about the normal to the underlying SrO. In order to enhance the depth resolution, the same samples were also measured in the glancing-exit geometry (scattering angle =95°).[8-9] As a result, an enhanced depth resolutional spectrum for near-surface of the top-Si layer was obtained. The minimum yield of the top-Si layer behind the surface peak was 0.027. This value is comparable to that for bulk Si.

4. Conclusion

In conclusion, SrO has been proposed for use as an insulating film with low dielectric constant(3.0) for a Si/insulator/Si hetero-epitaxial structure. Single crystalline SrO films were grown epitaxially on Si substrates by MBE. The orientation relationships between SrO and Si were confirmed to be (111)SrO//(111)Si and [1$\bar{1}$0]SrO//[$\bar{1}$10]Si (Type B), (100)SrO//(100)Si and [011]SrO//[001]Si. These films had a high breakdown field (5X10^6 V/cm). Futhermore, an epitaxial Si/insulator/Si stacked structure can be formed by MBE of Si on SrO/Si(111) structure. In addition, interdiffusion at the top-Si/SrO interfaces can be effectively reduced by introducing a 2000-3000 Å thick SPE layer. High crystalline quality Si comparable to bulk Si by RBS/C measurement has been obtained on the upper side of the top Si layer.

Acknowledgement

The authors are particulary indebted to Drs.M.Kondo, N.Ohwada and T.Sakai for their continued encouragements throughout the course of this work. They also wish to thank Mr.M.Takahashi for use of the Van de Graff accelerator and Dr.H.Okamoto for AES analysis.

References

1) M.Takigawa,M.Hirayama, and K.Shono, Japan.J.Appl.Phys.13(1974)411.

2)M.Ihara et al.,J.Electrochem.Soc.129(1982)2569.

3) H.Ishiwara and T.Asano, Appl. Phys. Lett. 40-1(1982)66.

4)Y.S.Touloukian,Thermophysical Properties of High Temperature Solid Materials, Vols.1to6, Macmillian, New York,(1967)

5)Primak et al.,J.Am.Chem.Soc.70(1948)2034.

6)M.Tabe, K.Arai and H.Nakamura, Japan.J.Appl.Phys. 20(1981)703.

7)R.T.Tung et al.,Appl.Phys.Lett. 40(1982)684.

8)J.S.Williams, Nucl.Instr.and Meth.126 (1975)205.

9)W.K.Chu, J.W.Mayer and M-A.Nicolet, Backscattering spectrometry (Academic Press, New York, 1978)